entropy

Article

An Improved Calculation Formula of the Extended Entropic Chaos Degree and Its Application to Two-Dimensional Chaotic Maps

Kei Inoue

Faculty of Engineering, Sanyo-Onoda City University, 1-1-1 Daigaku-Dori, Sanyo-Onoda 756-0884, Yamaguchi, Japan; kinoue@rs.socu.ac.jp

Abstract: The Lyapunov exponent is primarily used to quantify the chaos of a dynamical system. However, it is difficult to compute the Lyapunov exponent of dynamical systems from a time series. The entropic chaos degree is a criterion for quantifying chaos in dynamical systems through information dynamics, which is directly computable for any time series. However, it requires higher values than the Lyapunov exponent for any chaotic map. Therefore, the improved entropic chaos degree for a one-dimensional chaotic map under typical chaotic conditions was introduced to reduce the difference between the Lyapunov exponent and the entropic chaos degree. Moreover, the improved entropic chaos degree was extended for a multidimensional chaotic map. Recently, the author has shown that the extended entropic chaos degree takes the same value as the total sum of the Lyapunov exponents under typical chaotic conditions. However, the author has assumed a value of infinity for some numbers, especially the number of mapping points. Nevertheless, in actual numerical computations, these numbers are treated as finite. This study proposes an improved calculation formula of the extended entropic chaos degree to obtain appropriate numerical computation results for two-dimensional chaotic maps.

Keywords: chaos; Lyapunov exponent; extended entropic chaos degree

check for updates

Citation: Inoue, K. An Improved Calculation Formula of the Extended Entropic Chaos Degree and Its Application to Two-Dimensional Chaotic Maps. *Entropy* **2021**, *23*, 1511. https://doi.org/10.3390/e23111511

Academic Editor: Fan Yang and Wenkai Hu

Received: 9 October 2021
Accepted: 11 November 2021
Published: 14 November 2021

1. Introduction

The Lyapunov exponent (LE) is a widely used measure for quantifying the chaos of a dynamical system. However, it is generally incomputable for time series. Therefore, some estimation methods for the Lyapunov exponent of a time series have been suggested in previous studies [1–6]. However, it is well-known that estimating the Lyapunov exponent for a time series is difficult.

The entropic chaos degree (ECD) was introduced to measure the chaos of a dynamical system in the field of information dynamics [7]. The ECD is directly computable, even for time series data obtained from dynamical systems. Some researchers have sought to characterize certain chaotic behaviors using the ECD [8–10]. Recently, it was demonstrated that the modified ECD coincides with the Lyapunov exponent for a one-dimensional chaotic map under typical chaotic conditions [11,12]. Moreover, the extended entropic chaos degree (EECD) was shown to be the sum of all the Lyapunov exponents of a multidimensional chaotic map under typical chaotic conditions [13]. However, it was assumed that the number of mapping points and the number of all components of equipartition of the domain are infinity. In actual computations, these numbers are treated as finite numbers. In this study, I aim to formulate a calculation such that the EECD is also equal to the sum of all the Lyapunov exponents of two-dimensional typical chaotic maps in actual numerical computations.

In this study, I propose an improved calculation formula of the EECD for multidimensional chaotic maps. Moreover, I apply the improved calculation formula of the EECD to two-dimensional typical chaotic maps.

2. Entropic Chaos Degree

In this section, I briefly review the definition of the ECD for a difference equation system,

$$x_{n+1} = f(x_n),\ n = 0, 1, \ldots,$$

where f represents a map such that $f : I \to I\ (\equiv [a, b]^d \subset \mathbf{R}^d,\ a, b \in \mathbf{R},\ d \in \mathbf{N})$.

Let x_0 represent an initial value and $\{A_i\}$ represent a finite partition of I such that

$$I = \bigcup_{k=1}^{N} A_k,\quad A_i \cap A_j = \emptyset\ (i \neq j).$$

Next, the probability distribution $\left(p_{i,A}^{(n)}(M)\right)$ at time n and joint distribution $\left(p_{i,j,A}^{(n,n+1)}(M)\right)$ at time n and $n+1$ associated with the difference equation are expressed as follows:

$$\begin{aligned} p_{i,A}^{(n)}(M) &= \frac{1}{M}\sum_{k=n}^{n+M-1} 1_{A_i}(x_k) \\ &= \frac{|\{x_k \in A_i;\ n \leq k \leq n+M-1\}|}{M}, \\ p_{i,j,A}^{(n,n+1)}(M) &= \frac{1}{M}\sum_{k=n}^{n+M-1} 1_{A_i}(x_k) 1_{A_j}(x_{k+1}) \\ &= \frac{\left|\left\{(x_k, x_{k+1}) \in A_i \times A_j;\ n \leq k \leq n+M-1\right\}\right|}{M}, \end{aligned}$$

where 1_A represents the characteristic function of a set A.

The ECD D of the orbit $\{x_n\}$ is then defined in [7] as follows:

$$\begin{aligned} D^{(M,n)}(A, f) &= \sum_{i=1}^{N}\sum_{j=1}^{N} p_{i,j,A}^{(n)}(M) \log \frac{p_{i,A}^{(n)}(M)}{p_{i,j,A}^{(n,n+1)}(M)} \\ &= \sum_{i=1}^{N} p_{i,A}^{(n)}(M) \left(-\sum_{j=1}^{N} p_A^{(n)}(j|i)(M) \log p_A^{(n)}(j|i)(M) \right), \end{aligned} \tag{1}$$

where

$$p_A^{(n)}(j|i) \equiv \frac{p_{i,j,A}^{(n,n+1)}(M)}{p_{i,A}^{(n)}(M)}$$

represents the conditional probability from the component A_i of $\{A_i\}$ to the component A_j of $\{A_i\}$.

Further, the ECD is denoted as $D^{(M)}(A, f)$ without n if the orbit $\{x_n\}$ does not depend on time n. Moreover, the ECD is denoted as $D^{(M,n)}(A)$ without f if the map f does not produce the orbit $\{x_n\}$.

The ECD is larger than the Lyapunov exponent for a one-dimensional chaotic map [12].

At the end of this section, I discuss the relation between the ECD and the metric entropy. For sufficiently large M, there exists a probability measure μ on I without depending on n. Let (X, A, μ) be a measure space with $\mu(X) = 1$. For provided measurable partitions ξ and ζ of X, the conditional entropy $H_\mu(\xi|\zeta)$ of ξ with respect to ζ is defined in [14] by

$$H_\mu(\xi|\zeta) = -\sum_{C\in\xi, D\in\zeta} \mu(C \cap D) \log \frac{\mu(C \cap D)}{\mu(D)}. \tag{2}$$

If $T : I \to I$ is a measurable transformation preserving a probability measure μ on I then, for sufficiently large M, I have

$$\begin{aligned} D^{(M)}(\xi, T) &\simeq -\sum_{C\in\xi} \mu(C\cap T(C)) \log \frac{\mu(C\cap T(C))}{\mu(T(C))} \\ &= -\sum_{C\in\xi} \mu(C\cap T(C)) \log \frac{\mu(C\cap T(C))}{\mu(C)} \\ &= -\sum_{C\in\xi} \mu\left(T^{-1}(C\cap T(C))\right) \log \frac{\mu(T^{-1}(C\cap T(C)))}{\mu(T^{-1}(C))} \\ &= -\sum_{C\in\xi} \mu\left(T^{-1}(C)\cap C\right) \log \frac{\mu(T^{-1}(C)\cap C)}{\mu(T^{-1}(C))} \\ &= H_\mu\left(\xi \middle| T^{-1}\xi\right) \\ &\geq \lim_{n\to\infty} H_\mu\left(\xi \middle| \bigvee_{i=1}^{n} T^{-i}\xi\right). \end{aligned}$$

In the last inequality, I used the property such that if ζ is a refinement of η, then $H_\mu(\xi|\zeta) \leq H_\mu(\xi|\eta)$ for every partition ξ, where $\eta = T^{-1}\xi$ and $\zeta = \bigvee_{i=1}^{n} T^{-i}\xi$.

Then the metric entropy $h_\mu(T, \xi)$ of T with respect to μ and a measurable partition ξ has the following property [14].

$$h_\mu(T, \xi) = H_\mu\left(\xi \middle| \bigvee_{i=1}^{n} T^{-i}\xi\right).$$

Therefore, I obtain

$$D^{(M)}(\xi, T) \geq h_\mu(T, \xi)$$

for sufficiently large M.

3. Extended Entropic Chaos Degree

In this section, it is assumed that

$$N = L^d, \quad I = \prod_{l=1}^{d} [a_l, b_l]. \tag{3}$$

Let the L^d-equipartitions $\{A_i\}$ of I be

$$I = \bigcup_{k=0}^{L^d-1} A_k.$$

For any component A_i of $\{A_i\}$, I divide another component A_j into $\left(S_{i,j}\right)^d$-equipartitions $\left\{B_l^{(i,j)}\right\}_{0\leq l\leq (S_{i,j})^d-1}$ of smaller components, such that

$$A_j = \bigcup_{l=0}^{\left(S_{i,j}\right)^d-1} B_l^{(i,j)}. \tag{4}$$

For each $B_l^{(i,j)}$, the function $g_{i,j}$ is defined as follows:

$$g_{i,j}\left(B_l^{(i,j)}\right) = \begin{cases} 1 & (B_l^{(i,j)} \cap f(A_i) \neq \emptyset) \\ 0 & (B_l^{(i,j)} \cap f(A_i) = \emptyset) \end{cases} \tag{5}$$

Using the function $g_{i,j}$, for any two components A_i, A_j $(i \neq j)$ of the initial partition $\{A_i\}$, the function $R(S_{i,j})$ is defined as follows:

$$R(S_{i,j}) = \frac{\sum_{l=0}^{(S_{i,j})^d-1} g_{i,j}\left(B_l^{(i,j)}\right)}{\left(S_{i,j}\right)^d}.$$

The EECD D_S is provided in [13] as follows:

$$D_S^{(M,n)}(A,f) \quad = \quad \sum_{i=0}^{L^d-1} p_{i,A}^{(n)}(M) \sum_{j=0}^{L^d-1} p_A^{(n)}(j|i)(M) \log \frac{R(S_{i,j})}{p_A^{(n)}(j|i)(M)},$$

where $S = (S_{i,j})_{0 \leq i,j \leq L^d-1}$.

Note that the EECD D_S becomes the CD, as shown in Equation (1), only if $R(S_{i,j}) = 1$ for any two components A_i and A_j of the initial partition $\{A_i\}$.

First, the following theorem concerning the periodic orbit is presented [13].

Theorem 1. *Let L, M represent sufficiently large natural numbers. If map f creates a stable periodic orbit with period T, the following equality holds.*

$$D_S^{(M,n)}(A,f) = -\frac{d}{T} \sum_{k=1}^{T} \log S_{i_k,j_k}. \tag{6}$$

Second, I briefly review the relationship between the EECD and the Lyapunov exponent in a chaotic dynamical system. Let a map f be a piecewise C^1 function on $\mathbf{R}^d$. For any $\mathbf{x} = (x_1, x_2, \ldots, x_d)^t$, $\mathbf{y} = (y_1, y_2, \ldots, y_d)^t \in A_i$, I consider an approximate Jacobian matrix $\widehat{J}$ as follows:

$$\widehat{J}(\mathbf{x}, \mathbf{y}) = \left(\frac{f_i(\mathbf{x}) - f_i(\mathbf{y})}{x_j - y_j} \right)_{1 \leq i,j \leq d}.$$

Let $r_k(\mathbf{x}, \mathbf{y})$ $(k = 1, 2, \ldots, d)$ represent the eigenvalues of $\sqrt{\widehat{J}^t(\mathbf{x}, \mathbf{y})\widehat{J}(\mathbf{x}, \mathbf{y})}$.

Then, the following properties are assumed to be satisfied.

Assumption 1. *For sufficiently large natural numbers, L and M, I assume that the following conditions are satisfied.*

(1) Points in A_i are uniformly distributed over A_i.

(2) Then, $r_k(\mathbf{x}, \mathbf{y}) = r_k^{(i)}$, $k = 1, 2, \ldots, d$ is obtained for any $\mathbf{x}, \mathbf{y} \in A_i$.

Next, the following theorem is presented [13].

Theorem 2. *For any A_i, $i = 0, 1, \ldots, L^d - 1$, Assumption 1 is assumed to be satisfied. Then, the following is obtained.*

$$\lim_{S \to \infty} \lim_{L \to \infty} \lim_{M \to \infty} D_S^{(M,m)}(A,f) = \sum_{k=1}^{d} \lambda_k,$$

where

$$S \to \infty \Leftrightarrow S_{i,j} \to \infty \; (i,j = 0, 1, \ldots, L^d - 1)$$

and $\{\lambda_1, \ldots, \lambda_d\}$ represent the Lyapunov spectrum of a map f.

Theorem 2 implies that if the points on any A_i are uniformly distributed, then the EECD becomes the sum of all the Lyapunov exponents of the map f in the limits at infinity of M, L, and $S_{i,j}$.

At the end of this section, I discuss the relationship between the EECD and the metric entropy. For sufficiently large M, a probability measure μ exists on I without depending on n. If $T : I \to I$ is a measurable transformation preserving a probability measure μ on I, then for sufficiently large M and $S_{i,j}$, I have

$$\begin{aligned} D_S^{(M,n)}(\xi, T) &\simeq \sum_{C \in \xi} \mu(C \cap T(C)) \log \frac{\dfrac{m(C \cap T(C))}{m(C)}}{\dfrac{\mu(C \cap T(C))}{\mu(T(C))}} \\ &= \sum_{C \in \xi} \mu(C \cap T(C)) \log \frac{\dfrac{m(C \cap T(C))}{m(C)}}{\dfrac{m(C \cap T(C))}{m(C)}} \\ &= \sum_{C \in \xi} \mu(C \cap T(C)) \log 1 \\ &= 0. \end{aligned}$$

Here, m is the Lebesgue measure on R^d.

Because $h_\mu(T, \xi) \geq 0$, I have

$$D_S^{(M)}(\xi, T) \leq h_\mu(T, \xi)$$

for sufficiently large $M, S_{i,j}$.

4. Improvement of Calculation Formula of the Extended Entropic Chaos Degree

In Theorem 2, it is assumed that the values of L, M, and $S_{i,j}$ are equal to infinity. However, in actual numerical computations, these numbers are treated as finite numbers. I propose an improved calculation formula of the EECD to obtain appropriate numerical computation results.

First, I consider improving a calculation formula of the EECD when the map f creates a stable periodic orbit. If the map $f$creates a stable periodic orbit, then, for any component A_i with $A_i \neq \emptyset$, there exists a component A_{j_i} such that

$$|A_{j_i} \cap f(A_i)| = |f(A_i)| = |A_{j_i}|.$$

It follows that

$$p_A^{(n)}(j|i) = \begin{cases} 1 & (j = j_i) \\ 0 & (j \neq j_i) \end{cases}. \tag{7}$$

From Equation (7), I obtain

$$D_S^{(M,n)}(A, f) = \sum_{|A_i|>0} p_{i,A}^{(n)}(M) \log R(S_{i,j_i}).$$

Now, for any component A_i, let us consider A_j such that $A_j \cap f(A_i) \neq \emptyset$. Let $C_{i,j}$ be the number of $B_l^{(i,j)}$ such that $B_l^{(i,j)} \cap f(A_i) \neq \emptyset$, that is,

$$C_{i,j} \equiv \left| \left\{ B_l^{(i,j)} : \ (\mathbf{x}_k, f(\mathbf{x}_k)) \in A_i \times B_l^{(i,j)}, \ l = 0, 1, \ldots, (S_{i,j})^d - 1 \right\} \right|,$$

where
$$A_j = \bigcup_{l=0}^{(S_{i,j})^d - 1} B_l^{(i,j)}.$$
When the map f creates a stable periodic orbit, I set
$$(S_{i,j_i}) = \left\lfloor \sqrt[d]{|A_i|} \right\rfloor.$$
I then have
$$R(S_{i,j_i}) = \frac{C_{i,j}}{(S_{i,j_i})^d} \simeq \frac{1}{|A_i|} \simeq \frac{|\{A_i : |A_i| > 0\}|}{M}.$$
Thus, when the map f creates a stable periodic orbit, I use
$$\begin{aligned}\widetilde{D}_{S,1}^{(M,n)}(A,f) &\equiv \sum_{|A_i|>0} p_{i,A}^{(n)}(M) \log \frac{|\{A_i : |A_i| > 0\}|}{M} \\ &= \log \frac{|\{A_i : |A_i| > 0\}|}{M}\end{aligned} \tag{8}$$
to calculate the EECD.

Second, I consider improving a calculation formula of the EECD when the map f does not create a periodic orbit. For any sufficiently large natural numbers, L and M, let us assume the conditions (1) and (2) in Assumption 1. Let m be the Lebesgue measure on $\mathbf{R}^d$ and μ be the invariant measure of f. Then, I obtain
$$\begin{aligned}D_S^{(M,n)}(A,f) &= \sum_{i=0}^{L^d-1} p_{i,A}^{(n)}(M) \left(\sum_{j=0}^{L^d-1} p_A^{(n)}(j|i)(M) \log \frac{R(S_{i,j})}{p_A^{(n)}(j|i)(M)} \right) \\ &\simeq \sum_{i=0}^{L^d-1} \mu(f(A_i)) \left(\sum_{j=0}^{L^d-1} \frac{\mu(A_j \cap f(A_i))}{\mu(f(A_i))} \log \frac{\frac{m(A_j \cap f(A_i))}{m(A_j)}}{\frac{\mu(A_j \cap f(A_i))}{\mu(f(A_i))}} \right) \\ &\simeq \sum_{i=0}^{L^d-1} \sum_{j=0}^{L^d-1} \mu(A_j \cap f(A_i)) \log \frac{m(f(A_i))}{m(A_j)}.\end{aligned} \tag{9}$$
Here, the second approximation (Equation (9)) uses the following:
$$\frac{\mu(A_j \cap f(A_i))}{\mu(f(A_i))} \simeq \frac{m(A_j \cap f(A_i))}{m(f(A_i))}.$$
Then, I directly obtain the following:
$$\begin{aligned}&\sum_{i=0}^{L^d-1} \sum_{j=0}^{L^d-1} \mu(A_j \cap f(A_i)) \log \frac{m(f(A_i))}{m(A_j)} \\ &= \sum_{i=0}^{L^d-1} \mu(f(A_i)) \log m(f(A_i)) - \sum_{j=0}^{L^d-1} \mu(A_j) \log m(A_j) \\ &\simeq \sum_{i=0}^{L^d-1} p_{i,A}^{(n)}(M) \log m(f(A_i)) - \sum_{i=0}^{L^d-1} p_{i,A}^{(n)}(M) \log m(A_i) \\ &= \sum_{i=0}^{L^d-1} p_{i,A}^{(n)}(M) \log \frac{m(f(A_i))}{m(A_i)}.\end{aligned} \tag{10}$$

Now, for any set $X\ (\neq \emptyset) \subset I = \prod_{k=1}^{d} [a_k, b_k]$,

$$
\begin{aligned}
X &= \{(x_1, x_2, \ldots, x_d) :\ x_k \in [a_k, b_k], k = 1, 2, \ldots, d\} \\
&= \{((x_1)_j, (x_2)_j, \ldots, (x_d)_j) :\ (x_k)_j \in [a_k, b_k], k = 1, 2, \ldots, d, j = 0, 1, \ldots, |X| - 1\}.
\end{aligned}
$$

The variance–covariance matrix $\sum_X$ to all points $\mathbf{x}$ on X is given by

$$
\sum_X = \begin{pmatrix} (\sigma_1^2)_X & (\sigma_{1,2})_X & \cdots & (\sigma_{1,d})_X \\ (\sigma_{2,1})_X & (\sigma_2^2)_X & \cdots & (\sigma_{2,d})_X \\ \vdots & \vdots & \ddots & \vdots \\ (\sigma_{d,1})_X & (\sigma_{d,2})_X & \cdots & (\sigma_d^2)_X \end{pmatrix},
$$

where

$$
\begin{aligned}
(\sigma_{l,m})_X &= \frac{1}{|X|} \sum_{j=0}^{|X|-1} ((x_l)_j - \overline{x}_l)((x_m)_j - \overline{x}_m), \\
(\sigma_l^2)_X &= \frac{1}{|X|} \sum_{j=0}^{|X|-1} ((x_l)_j - \overline{x}_l)^2, \\
(\overline{x}_l)_X &= \frac{1}{|X|} \sum_{j=0}^{|X|-1} (x_l)_j.
\end{aligned}
$$

Let $(\lambda_k)_X$ $(k = 1, 2, \ldots, d)$ be eigenvalues of $\sum_X$ such that $(\lambda_i)_X \geq (\lambda_j)_X$ $(i \geq j)$. For any sufficiently large natural numbers, L and M, I have

$$
\frac{m(f(A_i))}{m(A_i)} \simeq \frac{2^d \prod_{k=1}^{d} \sqrt{(\lambda_k)_{f(A_i)}}}{2^d \prod_{k=1}^{d} \sqrt{(\lambda_k)_{A_i}}} = \frac{\prod_{k=1}^{d} \sqrt{(\lambda_k)_{f(A_i)}}}{\prod_{k=1}^{d} \sqrt{(\lambda_k)_{A_i}}}. \tag{11}
$$

From Equations (10) and (11), when the map f does not create a periodic orbit, I use

$$
\widetilde{D}_{S,2}^{(M,n)}(A, f) \equiv \sum_{|A_i|>0} p_{i,A}^{(n)}(M) \log \frac{\prod_{k=1}^{d} \sqrt{(\lambda_k)_{f(A_i)}}}{\prod_{k=1}^{d} \sqrt{(\lambda_k)_{A_i}}} \tag{12}
$$

as the calculation formula of the EECD.

Let $(\mathbf{u}_k)_X$ be the eigenvector corresponding to the eigenvalue $(\lambda_k)_X$, and

$$
\langle \mathbf{x} \rangle_X \equiv (\overline{x}_1, \overline{x}_2, \ldots, \overline{x}_d)_X.
$$

In actual numerical computations, let us consider subsets C_i, D_i of $A_i, f(A_i)$ such that

$$
\begin{aligned}
C_i &= \left\{ \langle \mathbf{x} \rangle_{A_i} + \sum_{k=1}^{d} \alpha_k \sqrt{(\lambda_k)_{A_i}} \frac{(\mathbf{u}_k)_{A_i}}{\|(\mathbf{u}_k)_{A_i}\|} :\ -1 \leq \alpha_k \leq 1 \right\}, && (13) \\
D_i &= \left\{ \langle \mathbf{x} \rangle_{f(A_i)} + \sum_{k=1}^{d} \beta_k \sqrt{(\lambda_k)_{f(A_i)}} \frac{(\mathbf{u}_k)_{f(A_i)}}{\left\|(\mathbf{u}_k)_{f(A_i)}\right\|} :\ -1 \leq \beta_k \leq 1 \right\}. && (14)
\end{aligned}
$$

Now, I assume that all points $\mathbf{x}$ on $A_i, f(A_i)$ are almost uniformly distributed over C_i, D_i, such that

$$\frac{|E_i|}{|C_i|} \simeq \frac{m(E_i)}{m(C_i)}, \quad \frac{|F_i|}{|D_i|} \simeq \frac{m(F_i)}{m(D_i)}$$

for any subsets E_i, F_i of C_i, D_i. Then, I obtain

$$\frac{m(f(C_i))}{m(C_i)} = \frac{m(D_i)}{m(C_i)} \simeq \frac{2^d \prod_{k=1}^{d} \sqrt{(\lambda_k)_{f(A_i)}}}{2^d \prod_{k=1}^{d} \sqrt{(\lambda_k)_{A_i}}} = \frac{\prod_{k=1}^{d} \sqrt{(\lambda_k)_{f(A_i)}}}{\prod_{k=1}^{d} \sqrt{(\lambda_k)_{A_i}}}. \tag{15}$$

Moreover, I denote the eigenvalues of $\sqrt{Df^t(\mathbf{x})Df(\mathbf{x})}$ such that $r_i(\mathbf{x}) \geq r_j(\mathbf{x})$ $(i \geq j)$ by $r_k(\mathbf{x})$ $(k = 1, 2, \ldots, d)$. Then, I have

$$\begin{aligned}
\widetilde{D}_{S,2}^{(M,n)}(A, f) &\simeq \sum_{|C_i|>0} p_{i,A}^{(n)}(M) \log \frac{m(f(C_i))}{m(C_i)} \\
&= \sum_{|C_i|>0} \int_{C_i} \log\left(\prod_{k=1}^{d} r_k(\mathbf{x})\right) p(\mathbf{x}) \prod_{l=1}^{d} dx_l \\
&= \int_{a_1}^{b_1} \int_{a_2}^{b_2} \cdots \int_{a_d}^{b_d} \log\left(\prod_{k=1}^{d} r_k(\mathbf{x})\right) p(\mathbf{x}) \prod_{l=1}^{d} dx_l \\
&= \sum_{k=1}^{d} \int_{a_1}^{b_1} \int_{a_2}^{b_2} \cdots \int_{a_d}^{b_d} \log(r_k(\mathbf{x})) p(\mathbf{x}) \prod_{l=1}^{d} dx_l \\
&= \sum_{k=1}^{d} \lambda_k.
\end{aligned} \tag{16}$$

Here, $p(\mathbf{x})$ is the density function of $\mathbf{x}$ and $\{\lambda_1, \lambda_2, \ldots, \lambda_d\}$ is the Lyapunov spectrum of f.

In the sequel, I use

$$\widetilde{D}_{S}^{(M,n)}(A, f) \equiv \begin{cases} \widetilde{D}_{S,1}^{(M,n)}(A, f) & \text{(when the map } f \text{ creates a stable periodic orbit)} \\ \widetilde{D}_{S,2}^{(M,n)}(A, f) & \text{(otherwise)} \end{cases} \tag{17}$$

as the calculation formulas of the EECD.

5. Numerical Computation Results of the EECD for Two-Dimensional Chaotic Maps

In this section, I apply the improved calculation formulas (Equation (12)) of the EECD to two-dimensional typical chaotic maps. In the sequel, I set M = 1,000,000 and $L = \sqrt{M} = 1000$. (In principle, the double type in C language is used in numerical computations. However, the floating-point type with its 1024-bit mantissa is used in numerical calculations of eigenvalues of the variance–covariance matrix by GMP (GNU Multi-Precision Library).)

Let us consider the generalized baker's map f_a as a simple two-dimensional dissipative chaotic map such that the Jacobian matrix $Df_a(\mathbf{x})$ does not depend on $\mathbf{x}$.

The generalized baker's map f_a is defined by

$$f_a(\mathbf{x}) = \begin{cases} \left(2ax_1, \frac{1}{2}ax_2\right) & \left(0 \leq x_1 \leq \frac{1}{2}\right) \\ \left(a(2x_1 - 1), \frac{1}{2}a(x_2 + 1)\right) & \left(\frac{1}{2} < x_1 \leq 1\right), \end{cases} \tag{18}$$

where $\mathbf{x} = (x_1, x_2)^t \in [0,1] \times [0,1]$ and $0 \leq a \leq 1$.

The generalized baker's map f_a for $0.5 \leq a \leq 1.0$ corresponds to the following operations: first, the unit square is stretched $2a$ times in the x_1 direction and compressed $a/2$ times in the x_2 direction; second, the right part protruding from the unit square is cut vertically and stacked on the top of the left part. The first operation is called "stretching" and the second operation is called "folding". These two operations are essential basic elements for producing chaotic behaviors.

5.1. Numerical Computation Results of the EECD for Generalized Baker's Map

The Jacobian matrix of the baker's map f_a is expressed as follows:

$$Df_a(\mathbf{x}) = \begin{pmatrix} 2a & 0 \\ 0 & \frac{1}{2}a \end{pmatrix}. \tag{19}$$

Thus, $Df_a(\mathbf{x})$ depends only on the parameter a. The dynamics produced by the baker's map f_a is dissipative for $0 \leq a < 1$ because $|\mathrm{det} Df_a(\mathbf{x})| = a^2$.

For $\mathbf{e}_1 = (1,0)^t,\ \mathbf{e}_2 = (0,1)^t$, I obtain

$$\hat{\mathbf{e}}_1 \equiv Df_a(\mathbf{e}_1)\mathbf{e}_1 = 2a\mathbf{e}_1, \quad \hat{\mathbf{e}}_2 \equiv Df_a(\mathbf{e}_2)\mathbf{e}_2 = \frac{1}{2}a\mathbf{e}_2. \tag{20}$$

Thus, the expansion rate in the stretching of the baker's map f_a is $2a$ and the contraction rate in the folding of the baker's map f_a is $a/2$. I then consider the orbit $\{\mathbf{x}_n\}$ produced by the generalized baker's map f_a, as follows:

$$\mathbf{x}_{n+1} = f_a(\mathbf{x}_n),\ n = 0, 1, 2, \ldots, \mathbf{x_0} = (0.3333, 0.3333)^t.$$

First, I present typical orbits of the baker's map f_a in Figure 1. As the parameter a increases, the spread of points is mapped from a linear distribution to the entire unit square.

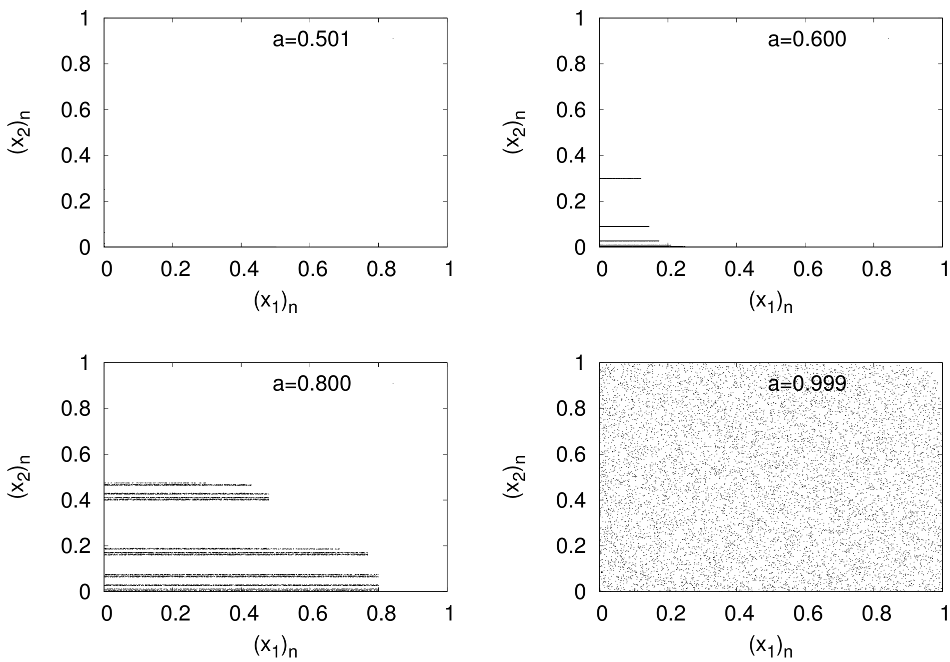

Figure 1. $(x_2)_n$ versus $(x_1)_n$ for the generalized baker's map f_a.

Second, I present the numerical computation results of the LEs λ_1, λ_2 $(\lambda_1 > \lambda_2)$, the total sum $\lambda_1 + \lambda_2$ of the LEs, the ECD D, and the EECD $\widetilde{D}_S$ of the baker's map f_a in

Figure 2. Figure 2 shows that the EECD $\widetilde{D}_S$ takes approximately the exact value of the total sum $\lambda_1 + \lambda_2$ of the LEs for the generalized baker's map f_a.

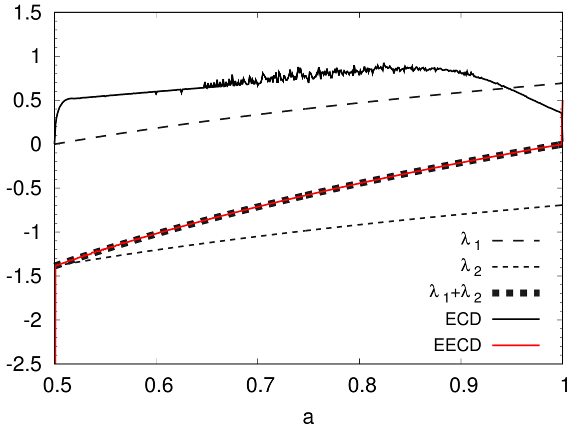

Figure 2. λ_1, λ_2, $\lambda_1 + \lambda_2$, D, $\widetilde{D}_S$ versus a for the generalized baker's map f_a.

In general, the orthogonal basis of $\mathbf{R}^d$ can be changed by f. In the sequel, for a two-dimensional chaotic map f, I consider the average expansion rate in the stretching of f as $\exp(\lambda_1)$ and the average contraction rate in the folding of f as $\exp(\lambda_2)$, where λ_1, λ_2 are the LEs of f such that $\lambda_1 > 0 > \lambda_2$.

5.2. Numerical Computation Results of the EECD for Tinkerbell Map

Let us consider the Tinkerbell map f_a as a two-dimensional dissipative chaotic map such that the Jacobian matrices $Df_a(\mathbf{x})$ and $\det Df_a(\mathbf{x})$ depend on $\mathbf{x}$ and the parameter a.

The Tinkerbell map f_a is defined by

$$f_a(\mathbf{x}) = \left(x_1^2 - x_2^2 + ax_1 - 0.6013x_2, 2x_1x_2 + 2x_1 + 0.5x_2\right)^t, \tag{21}$$

where $\mathbf{x} = (x_1, x_2)^t \in [a_1, b_1] \times [a_2, b_2]$.

For $0.7 \le a \le 0.9$, I obtain the following:

$$a_1 = -1.3, \quad a_2 = -1.6, \quad b_1 = 0.5, \quad b_2 = 0.6.$$

The Jacobian matrix of the Tinkerbell map f_a is expressed as follows:

$$Df_a(\mathbf{x}) = \begin{pmatrix} 2x_1 + a & -2x_2 - 0.6013 \\ 2x_2 + 2 & 2x_1 + 0.5 \end{pmatrix}. \tag{22}$$

Thus, $Df_a(\mathbf{x})$ depends on $\mathbf{x}$ and the parameter a.

I then consider the orbit $\{\mathbf{x}_n\}$ produced by the Tinkerbell map f_a as follows:

$$\mathbf{x}_{n+1} = f_a(\mathbf{x}_n), \, n = 0, 1, 2, \ldots, \mathbf{x_0} = (0.1, 0.1)^t.$$

First, I present typical orbits of the Tinkerbell map f_a in Figure 3. The orbit of the Tinkerbell map f_a constructs a strange attractor at $a = 0.9$. The map f_a is named the Tinkerbell map because the shape of the attractor produced by the Tinkerbell map looks like the movement of a fairy named Tinker Bell, who appears in a Disney film.

Second, I present the numerical computation results of the LEs λ_1, λ_2 ($\lambda_1 > \lambda_2$), the total sum $\lambda_1 + \lambda_2$ of the LEs, the ECD D, and the EECD $\widetilde{D}_S$ of the Tinkerbell map f_a in Figure 4. Figure 4 shows that the EECD $\widetilde{D}_S$ takes almost the same value as the total sum $\lambda_1 + \lambda_2$ of the LEs for the Tinkerbell map f_a at most a for $0.7 \le a \le 0.9$. However, the Tinkerbell map f_a creates a stable periodic orbit at several a's. Then the EECD takes a different value from the total sum $\lambda_1 + \lambda_2$ of LEs for the Tinkerbell map f_a because I use $\widetilde{D}^{(M,n)}_{S,1}$(Equation (8)) as the calculation formula of the EECD $\widetilde{D}_S$.

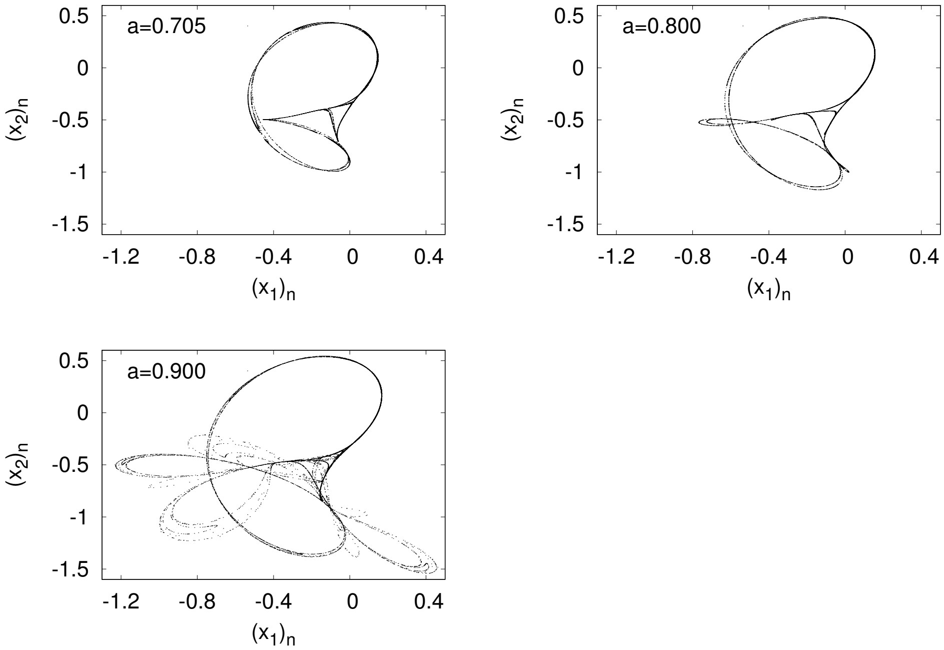

Figure 3. $(x_2)_n$ versus $(x_1)_n$ for the Tinkerbell map f_a.

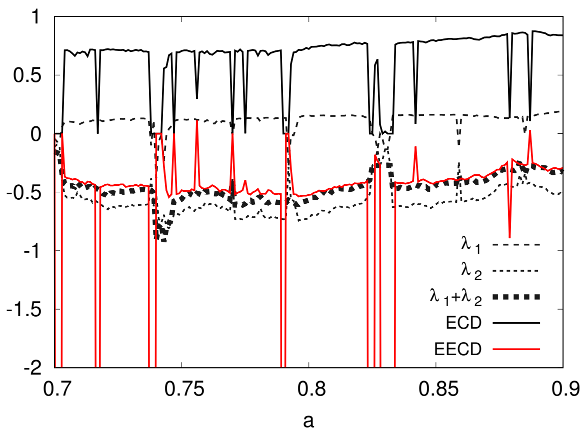

Figure 4. $\lambda_1, \lambda_2, \lambda_1 + \lambda_2$, D, $\widetilde{D}_S$ versus a for the Tinkerbell map f_a.

5.3. Numerical Computation Results of the EECD for Ikeda Map

Let us consider the Ikeda map f_a as a two-dimensional dissipative chaotic map such that the Jacobian matrix $Df_a(\mathbf{x})$ depends on $\mathbf{x}$ and the parameter a but that $\det Df_a(\mathbf{x})$ does not depend on $\mathbf{x}$.

The modified Ikeda map is given as the complex map in [15,16]

$$f(z) = A + Bze^{iK/(|z|^2+1)+C}, \quad z \in \mathbf{C}, \quad A, B, K, C \in \mathbf{R}. \tag{23}$$

The Ikeda map f_a is defined as a real two-dimensional example of Equation (23) by

$$f_a(\mathbf{x}) = (1 + a(x_1 \cos t - x_2 \sin t), a(x_1 \sin t + x_2 \cos t))^t, \tag{24}$$

where

$$t = 0.4 - \frac{6}{1 + x_1^2 + x_2^2}$$

and $\mathbf{x} = (x_1, x_2)^t \in [a_1, b_1] \times [a_2, b_2]$.

For $0.7 \leq a \leq 0.9$, I obtain the following:

$$a_1 = -0.4, \quad a_2 = -2.3, \quad b_1 = 1.8 \quad , b_2 = 0.9.$$

The Jacobian matrix of the Ikeda map f_a is expressed as follows:

$$Df_a(\mathbf{x}) = a \begin{pmatrix} u_1 \cos t - u_2 \sin t & -u_3 \sin t - u_4 \cos t \\ u_1 \sin t + u_2 \cos t & u_3 \cos t - u_4 \sin t \end{pmatrix}, \tag{25}$$

where

$$u_1 = 1 - \frac{12 x_1 x_2}{\left(1 + x_1^2 + x_2^2\right)^2}, \quad u_2 = \frac{12 x_1^2}{\left(1 + x_1^2 + x_2^2\right)^2}$$
$$u_3 = 1 + \frac{12 x_1 x_2}{\left(1 + x_1^2 + x_2^2\right)^2}, \quad u_4 = \frac{12 x_2^2}{\left(1 + x_1^2 + x_2^2\right)^2}.$$

Thus, $Df_a(\mathbf{x})$ depends on $\mathbf{x}$ and the parameter a. The dynamics produced by the Ikeda map f_a are dissipative for $0 \leq a < 1$ because $|\det Df_a(\mathbf{x})| = a^2$.

I then consider the orbit $\{\mathbf{x}_n\}$ produced by the Ikeda map f_a as follows:

$$\mathbf{x}_{n+1} = f_a(\mathbf{x}_n), \; n = 0, 1, 2, \ldots, \mathbf{x_0} = (0.1, 0.0)^t.$$

First, I present typical orbits of the Ikeda map f_a in Figure 5. As the parameter a increases, the attractor constructed by the Ikeda map f_a becomes larger. Regarding f_a plots, the Ikeda map might be conjugated to a Hénon map [17].

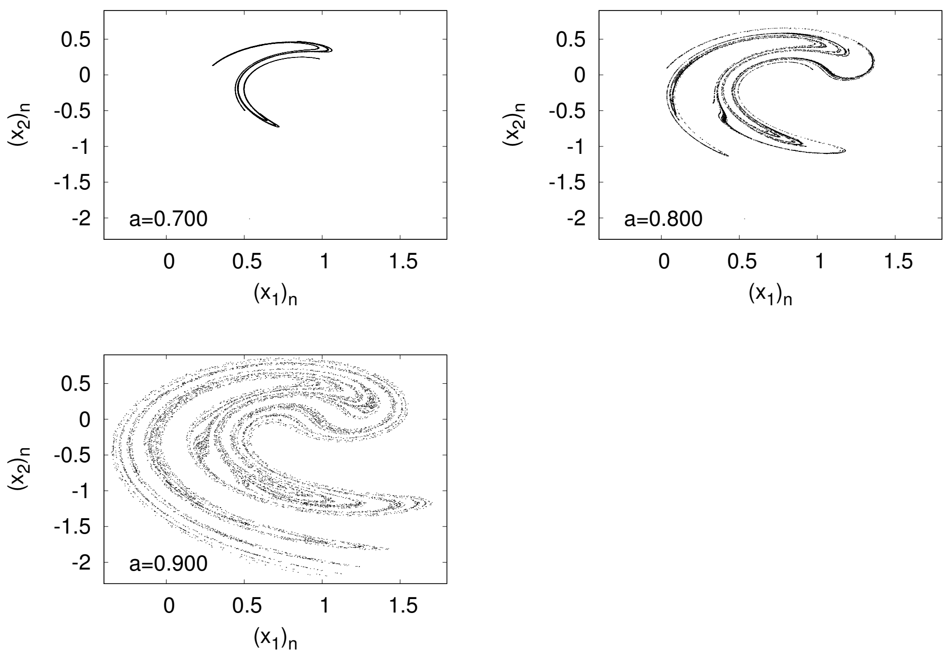

Figure 5. $(x_2)_n$ versus $(x_1)_n$ for the Ikeda map f_a.

Second, let us assume that dv_0 is transformed to dv_m by f_a^m on $\mathbf{R}^2$. For the Ikeda map f_a, using the chain rule and $\det Df_a(\mathbf{x}) = a^2$ at any $\mathbf{x}$, I have

$$dv_m = \det Df_a^m(\mathbf{v}_0) dv_0 = a^{2m} dv_0. \tag{26}$$

Therefore, I obtain

$$\lambda_1 + \lambda_2 = \lim_{m\to\infty} \frac{1}{m} \log\left|\frac{dv_m}{dv_0}\right| = \lim_{m\to\infty} \frac{\log a^{2m}}{m} = 2\log a, \tag{27}$$

where λ_k $(k = 1, 2)$ are the LEs of the Ikeda map f_a such that $\lambda_1 > \lambda_2$.

I present the numerical computation results of the LEs λ_1, λ_2, the total sum $\lambda_1 + \lambda_2$ of the LEs, the ECD D, and the EECD $\widetilde{D}_S$ of the Ikeda map f_a in Figure 6. Figure 6 shows that the EECD $\widetilde{D}_S$ takes almost the same value as the total sum $\lambda_1 + \lambda_2$ of the LEs for the Ikeda map f_a at almost a for $0.7 \leq a \leq 0.9$. However, the Ikeda map f_a creates a stable periodic orbit at several a's. Then the EECD takes a different value from the total sum $\lambda_1 + \lambda_2$ of LEs for the Ikeda map f_a because I use $\widetilde{D}_{S,1}^{(M,n)}$(Equation (8)) as the calculation formula of the EECD $\widetilde{D}_S$.

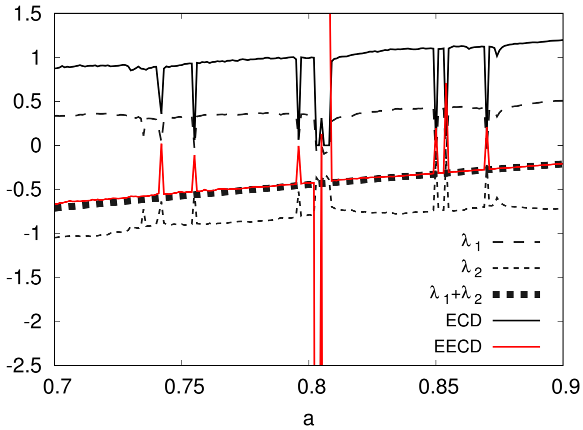

Figure 6. $\lambda_1, \lambda_2, \lambda_1 + \lambda_2$, D, $\widetilde{D}_S$ versus a for the Ikeda map f_a.

5.4. Numerical Computation Results of the EECD for Hénon Map

Let us consider the Hénon map $f_{a,b}$ as a two-dimensional dissipative chaotic map such that the Jacobian matrix $Df_{a,b}(\mathbf{x})$ depends on $\mathbf{x}$ and the parameter b but that the Jacobian $\det Df_{a,b}(\mathbf{x})$ does not depend on $\mathbf{x}$.

The Hénon map $f_{a,b}$ is expressed as follows:

$$f_{a,b}(\mathbf{x}) = \left(a - x_1^2 + bx_2, x_1\right)^t, \tag{28}$$

where $\mathbf{x} = (x_1, x_2)^t \in [a_1, b_1] \times [a_2, b_2]$.

For $a = 1.4, 0 < b \leq 0.3$, I obtain the following:

$$a_k = -1.8, \quad b_k = 1.8, \quad (k = 1, 2).$$

In the sequel, we rewrite $f_{1.4,b} = f_b$.

The Jacobian matrix of the Hénon map $f_{a,b}$ is expressed as follows:

$$Df_{a,b}(\mathbf{x}) = \begin{pmatrix} 2x_1 & b \\ 1 & 0 \end{pmatrix}. \tag{29}$$

Thus, $Df_{a,b}(\mathbf{x})$ depends on x_1 and the parameter b. The dynamics produced by the Hénon map $f_{a,b}$ are dissipative for $0 \leq b < 1$ because $|\det Df_{a,b}(\mathbf{x})| = b$.

I then consider the orbit $\{\mathbf{x}_n\}$ produced by the Hénon map f_b as follows:

$$\mathbf{x}_{n+1} = f_b(\mathbf{x}_n),\ n = 0, 1, 2, \ldots, \mathbf{x_0} = (0.1, 0.1)^t.$$

First, I present typical orbits of the Hénon map f_b in Figure 7. The orbit of the Hénon attractor has a fractal structure. Expanding a strip region, I find that innumerable parallel curves reappear in the strip.

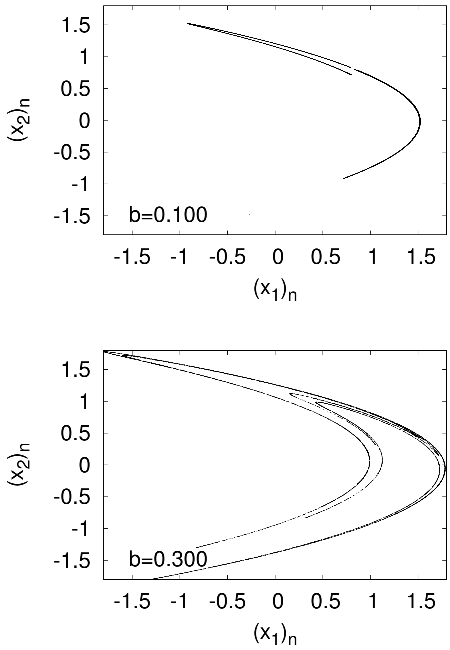

Figure 7. $(x_2)_n$ versus $(x_1)_n$ for the Hėnon map f_b.

Second, let us assume that dv_0 is transformed to dv_m by f_b^m on $\mathbf{R}^2$. For the Hénon map f_b, using the chain rule and $\det Df_b(\mathbf{x}) = -b$ at any $\mathbf{x}$, I have

$$dv_m = \det Df_b^m(\mathbf{v}_0)dv_0 = (-b)^m dv_0. \tag{30}$$

Therefore, I obtain

$$\lambda_1 + \lambda_2 = \lim_{m\to\infty} \frac{1}{m} \log\left|\frac{dv_m}{dv_0}\right| = \lim_{m\to\infty} \frac{\log b^m}{m} = \log b, \tag{31}$$

where λ_k $(k = 1, 2)$ are the LEs of the Hénon map f_b such that $\lambda_1 > \lambda_2$.

I present the numerical computation results of the LEs λ_1, λ_2 $(\lambda_1 > \lambda_2)$, the total sum $\lambda_1 + \lambda_2$ of the LEs, the ECD D, and the EECD $\widetilde{D}_S$ for the Hénon map f_b in Figure 8. Figure 8 shows that the EECD $\widetilde{D}_S$ takes a value almost equal to the total sum $\lambda_1 + \lambda_2$ of the LEs for the Hénon map f_b at most b for $0.1 < b \leq 0.3$. However, the EECD takes a different value from the total sum $\lambda_1 + \lambda_2$ of LEs for the Hénon map f_a, even though the Hénon map f_a does not create a periodic orbit at many bs for $0 < b \leq 0.1$. Here, the absolute value of the negative LE λ_2 is much larger than the absolute value of the positive LE λ_1.

Now, let ρ_{A_i} be the autocorrelation function to all points $\mathbf{x}$ on a component A_i. I consider the average of $|\rho_{A_i}|$ such that

$$E(|\rho|) = \sum_{|A_i|>3} \frac{|A_i|}{\sum\limits_{|A_i|>3} |A_i|} |\rho_{A_i}|. \tag{32}$$

I present the numerical computation results of the total sum $\lambda_1 + \lambda_2$ of the LEs, the EECD $\widetilde{D}_S$, and the average of $|\rho_{A_i}|$ for the Hénon map f_b in Figure 9.

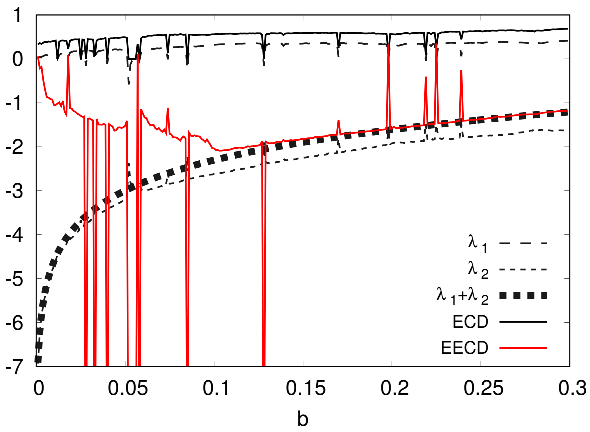

Figure 8. $\lambda_1, \lambda_2, \lambda_1 + \lambda_2$, D, $\widetilde{D}_S$ versus a for the Hėnon map f_b.

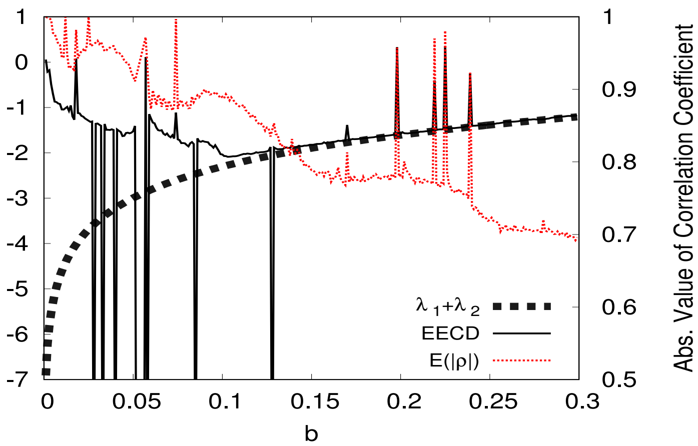

Figure 9. $\lambda_1 + \lambda_2$, $\widetilde{D}$, $E(|\rho|)$ versus a for the Hėnon map f_a.

Here, at $d = 2$, the denominator of the right side of Equation (11) is given by

$$\sqrt{(\lambda_1)_{A_i}(\lambda_2)_{A_i}}, \tag{33}$$

where $(\lambda_k)_{A_i}$ $(k = 1, 2)$ is the eigenvalue of the variance–covariance matrix $\sum_{A_i}$ to all points $\mathbf{x}$ on A_i.

Let $(\sigma_k^2)_{A_i}$ $(k = 1, 2)$ and $(\sigma_{1,2})_{A_i}$ be the variances and covariance of all points on A_i, respectively. Then, I have

$$\begin{aligned}
(\lambda_1)_{A_i} &= \frac{(\sigma_1^2)_{A_i} + (\sigma_2^2)_{A_i} + \sqrt{\{(\sigma_1^2)_{A_i} + (\sigma_2^2)_{A_i}\}^2 - 4(\sigma_1^2)_{A_i}(\sigma_2^2)_{A_i}\{1 - (\rho_{A_i})^2\}}}{2}, \\
(\lambda_2)_{A_i} &= \frac{(\sigma_1^2)_{A_i} + (\sigma_2^2)_{A_i} - \sqrt{\{(\sigma_1^2)_{A_i} + (\sigma_2^2)_{A_i}\}^2 - 4(\sigma_1^2)_{A_i}(\sigma_2^2)_{A_i}\{1 - (\rho_{A_i})^2\}}}{2}.
\end{aligned}$$

Therefore, if the absolute value of ρ_{A_i} is equal to 1, then I have

$$(\lambda_1)_{A_i} = (\sigma_1^2)_{A_i} + (\sigma_2^2)_{A_i}, \quad (\lambda_2)_{A_i} = 0. \tag{34}$$

Thus, it becomes difficult to estimate $m(f(A_i))/m(A_i)$ by Equation (11) when the absolute value of ρ_{A_i} is approximately 1. Therefore, the EECD takes a different value from the total sum of the LEs when $E(|\rho|)$ is near 1.

5.5. Numerical Computation Results of the EECD for Standard Map

Let us consider the standard map f_K as a two-dimensional conservative chaotic map such that the Jacobian matrix $Df_K(\mathbf{y})$ depends on $\mathbf{y}$ and the parameter K.

The standard map f_K is defined as follows:

$$f_K(\mathbf{y}) = (\theta + p + K\sin\theta,\ p + K\sin\theta)^t, \tag{35}$$

where $\mathbf{y} = (\theta, p)^t \in [-\pi, \pi]^2$.

The Jacobian matrix of the standard map f_K is expressed as follows:

$$Df_K(\mathbf{y}) = \begin{pmatrix} 1 + K\cos\theta & 1 \\ K\cos\theta & 1 \end{pmatrix}. \tag{36}$$

Thus, $Df_K(\mathbf{x})$ depends on θ and the parameter K. The dynamics produced by the standard map f_K become conservative because $|\det Df_K(\mathbf{x})| = 1$.

I then consider the orbit $\{\mathbf{y}_n\}$ produced by the standard map f_K as follows:

$$\mathbf{y}_{n+1} = f_K(\mathbf{y}_n),\ n = 0, 1, 2, \ldots, \mathbf{y_0} = (1.5, 2.0)^t.$$

First, I present typical orbits of the standard map f_K with initial point $(\theta_0, p_0) = (1.5, 2.0)$ in Figure 10.

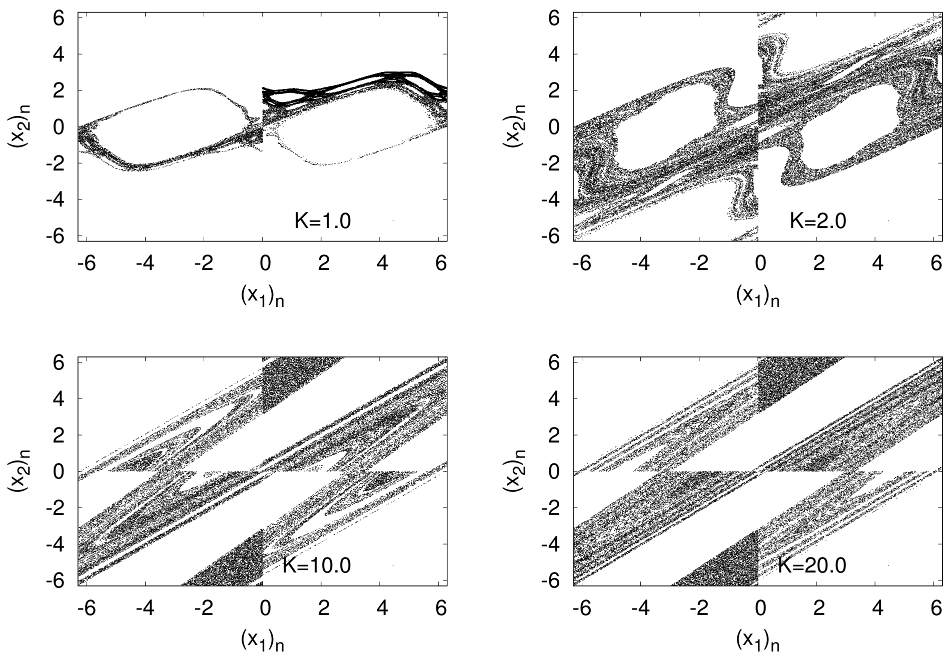

Figure 10. $(x_2)_n$ versus $(x_1)_n$ for the standard map f_K.

The standard map consists of the Poincaré's surface of the section of the kicked rotator. The map has a linear structure around $K = 0$. However, as K increases, the map produces a nonlinear structure and chaos for an appropriate initial condition.

Second, let us assume that dv_0 is transformed to dv_m by f_K^m on $\mathbf{R}^2$. For the standard map f_K, using the chain rule and $\det Df_K(\mathbf{x}) = 1$, I have

$$dv_m = \det Df_K^m(\mathbf{v}_0)dv_0 = dv_0. \tag{37}$$

Therefore, I obtain

$$\lambda_1 + \lambda_2 = \lim_{m\to\infty} \frac{1}{m} \log\left|\frac{dv_m}{dv_o}\right| = 0, \tag{38}$$

where λ_k $(k = 1, 2)$ are the LEs of the standard map f_K such that $\lambda_1 > \lambda_2$.

I present the numerical computation results of the LEs λ_1, λ_2 $(\lambda_1 > \lambda_2)$, the total sum $\lambda_1 + \lambda_2$ of the LEs, the ECD D, and the EECD $\widetilde{D}_S$ for the standard map f_K in Figure 11. Figure 11 shows that as K increases, the difference between the EECD $\widetilde{D}_S$ and the total sum $\lambda_1 + \lambda_2$ of LEs for the standard map f_b increases. In other words, as the positive LE increases, the difference between the EECD and the total sum of the LE increases.

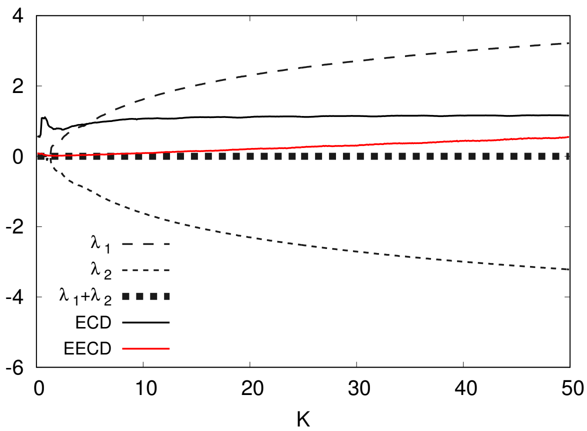

Figure 11. $\lambda_1, \lambda_2, \lambda_1 + \lambda_2$, D, $\widetilde{D}_S$ versus K for the standard map f_K.

Now, I consider symmetric difference equations such that

$$x_{n+1} + x_{n-1} = 2x_n + K \sin x_n. \quad (39)$$

Here, Equation (39) can arise as a discretization of $\frac{d^2}{dt^2}x = g(x) - 2x$ with $g(x) = 2x + K \sin x$ [18].

Introducing new variables $\theta_n \equiv x_n$, $p_n \equiv x_n - x_{n-1}$, Equation (39) can be written as

$$\begin{aligned} \theta_{n+1} &= \theta_n + p_n + K \sin \theta_n, \\ p_{n+1} &= p_n + K \sin \theta_n. \end{aligned} \quad (40)$$

This mapping is equivalent to the standard map Equation (35).

Moreover, let R be an involution such that $R(x_n, x_{n-1}) = (x_{n-1}, x_n)$. Then, I have

$$R(\theta_n, p_n) = (\theta_n - p_n, -p_n). \quad (41)$$

Using $(R \circ f)^2 = id$ and $R^2 = id$, I obtain

$$R \circ f = f^{-1} \circ R, \quad (42)$$

which signifies that the standard map f_K is reversible with respect to the involution R.

Equation (40) is area preserving as well as reversible, as is common with area-preserving maps [19]. Since the standard map f_k is reversible, two Lyapunov exponents of f_K become λ_1 and λ_2 such that $\lambda_1 = -\lambda_2 > 0$ by Theorem 3.2 in [20].

Let us consider increasing and decreasing L of the EECD. I represent the numerical computation results of the EECD at $L = 500, 1000, 2000$ for the standard map f_a in Figure 12. Figure 12 shows that as L increases, the EECD $\widetilde{D}_S$ goes to the total sum $\lambda_1 + \lambda_2$ of the LEs for the standard map f_K.

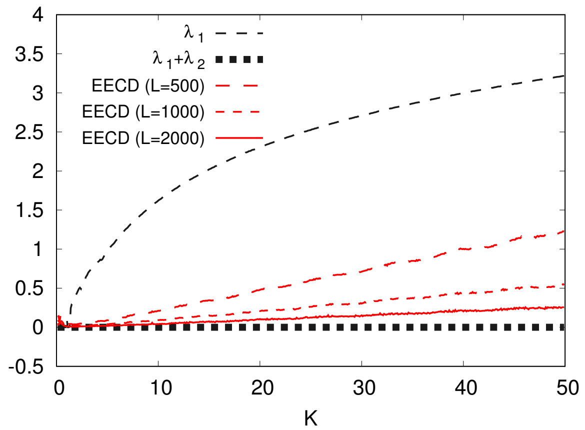

Figure 12. λ_1, $\lambda_1 + \lambda_2$, $\widetilde{D}_S$ at several Ls versus K for the standard map f_K.

6. Conclusions

In this study, I have focused on improving the calculation formula of the EECD and applied the improved calculation formula of the EECD to two-dimensional typical chaotic maps. I have shown that the EECD is almost equal to the total sum of the LEs for their chaotic maps in many cases. However, for the two cases, the EECD was different from the total sum of the LEs even though the map did not create a periodic orbit.

The first case occurs when the absolute value of the negative LE is much larger than the absolute value of the positive LE. Evidently, for the Hénon map f_a, the EECD takes a much larger value than the total sum of the LE at many a's for $0 < a \leq 0.1$. Then, the average $E(|\rho|)$ of the absolute value of the autocorrelation function ρ_{A_i} to all points on component A_i was approximately one. Here, it becomes difficult to estimate $m(f(A_i))/m(A_i)$ by Equation (11). Therefore, the EECD takes a different value from the total sum of the LEs when $E(|\rho|)$ is approximately one.

The second case occurs notably when the positive LE takes a large value. Evidently, for the standard map f_K, as the parameter K increases, the difference between the EECD and the total sum of the LE increases. In other words, as the positive LE increases, the difference between the EECD and the total sum of the LEs also increases. Here, I have shown the possibility of reducing the above difference by increasing L, where L^2 is the number of equipartitions $\{A_i\}$ of $I = [-\pi, \pi]^2$.

I have applied the improved calculation formulas of the EECD to two-dimensional chaotic maps. However, in future works, I will discuss applying the improved calculation formulas of the EECD to higher-dimensional chaotic dynamics.

Funding: This research received no external funding.

Institutional Review Board Statement: Not applicable.

Informed Consent Statement: Not applicable.

Data Availability Statement: Not applicable.

Acknowledgments: The author is very grateful to the referees for their helpful comments and suggestions. This work was supported by JSPS KAKENHI Grant Number 21K12063.

Conflicts of Interest: The authors declare no conflict of interest.

References

1. Eckmann, J.P.; Kamphorst, S.O.; Ruelle, D.; Ciliberto, S. Lyapunov exponents from time series. *Phys. Rev. A* **1986**, *34*, 4971–4979. [CrossRef] [PubMed]
2. Rosenstein, M.T.; Collins, J.J.; De Luca, C.J. A practical method for calculating largest Lyapunov exponents from small data sets. *Phys. D: Nonlinear Phenom.* **1993**, *65*, 117–134. [CrossRef]
3. Sato, S.; Sano, M.; Sawada, Y.; Practical methods of measuring the generalized dimension and the largest Lyapunov exponent in high dimensional chaotic systems. *Prog. Theor. Phys.* **1987**, *77*, 1–5. [CrossRef]

4. Sano, M.; Sawada, Y. Measurement of the Lyapunov spectrum from a chaotic time series. *Phys. Let. A* **1995**, *209*, 327–332. [CrossRef] [PubMed]
5. Wright, J. Method for calculating a Lyapunov exponent. *Phys. Rev. A* **1984**, *29*, 2924–2927. [CrossRef]
6. Wolf, A.; Swift, J.B.; Swinney, H.L.; Vastano, J.A. Determining Lyapunov exponents from a time series. *Phys. D Nonlinear Phenom.* **1985**, *16D*, 285–317. [CrossRef]
7. Ohya, M. Complexities and their applications to characterization of chaos. *Int. J. Theor. Phys.* **1998**, *37*, 495–505. [CrossRef]
8. Inoue, K.; Ohya, M.; Sato, K. Application of chaos degree to some dynamical systems. *Chaos Solitons Fractals* **2000**, *11*, 1377–1385. [CrossRef]
9. Inoue, K.; Ohya, M.; Volovich, I. Semiclassical properties and chaos degree for the quantum baker's map. *J. Math. Phys.* **2002**, *43*, 734–755. [CrossRef]
10. Inoue, K.; Ohya, M.; Volovich, I. On a combined quantum baker's map and its characterization by entropic chaos degree. *Open Syst. Inf. Dyn.* **2009**, *16*, 179–194. [CrossRef]
11. Mao, T.; Okutomi, H.; Umeno, K. Investigation of the difference between Chaos Degree and Lyapunov exponent for asymmetric tent maps. *JSIAM Lett.* **2019**, *11*, 61–64. [CrossRef]
12. Mao, T.; Okutomi, H.; Umeno, K. Proposal of improved chaos degree based on interpretation of the difference between chaos degree and Lyapunov exponent. *Trans. JSIAM* **2019**, *29*, 383–394. (In Japanese)
13. Inoue, K.; Mao, T.; Okutomi, H.; Umeno, K. An extension of the entropic chaos degree and its positive effect. *Jpn. J. Ind. Appl. Math.* **2021**, *38*, 611–624. [CrossRef]
14. Barreira, L. *Ergodic Theory, Hyperbolic Dynamics and Dimension Theory*; Springer: Berlin/Heidelberg, Germany, 2012.
15. Ikeda, K; Multiple-valued stationary state and its instability of the transmitted light by a ring cavity system. *Opt. Commun.* **1979**, *30*, 257–261. [CrossRef]
16. Ikeda, K.; Daido, H.; Akimoto, O. Optical Turbulence: Chaotic Behavior of Transmitted Light from a Ring Cavity. *Phys. Rev. Lett.* **1980**, *45*, 709–712. [CrossRef]
17. Wang, Q.; Oksasoglu, A. Rank one chaos: Theory and applications. *Int. J. Bifurc. Chaos* **2008**, *18*, 1261–1319. [CrossRef]
18. Lamb, J.S.W.; Roberts, A.G. Time-reversal symmetry in dynamical systems: A survey. *Phys. D* **1998**, *112*, 1–39. [CrossRef]
19. Roberts, J.A.G.; Quispel, G.R.W. Chaos and time-reversal symmetry. Order and chaos in reversible dynamical systems. *Phys. Rep.* **1992**, *216*, 63–177. [CrossRef]
20. Bessa, M.; Carvalho, M.; Rodrigues, A. Generic area-preserving reversible diffeomorphisms. *Nonlinearity* **2015**, *28*, 1695–1720. [CrossRef]